Journal of Applied Physics

RESEARCH ARTICLE | JANUARY 25 2024

Epitaxial growth of $AgCrSe_2$ thin films by molecular beam epitaxy

Y. Nanao ; C. Bigi ; A. Rajan ; G. Vinai ; D. Dagur ; P. D. C. King

J. Appl. Phys. 135, 045303 (2024)
https://doi.org/10.1063/5.0184273

Journal of Applied Physics ARTICLE pubs.aip.org/aip/jap

Epitaxial growth of $AgCrSe_2$ thin films by molecular beam epitaxy

Cite as: J. Appl. Phys. **135**, 045303 (2024); doi: 10.1063/5.0184273
Submitted: 2 November 2023 · Accepted: 22 December 2023 ·
Published Online: 25 January 2024

View Online Export Citation CrossMark

Y. Nanao,[1,a)] C. Bigi,[1,b)] A. Rajan,[1] G. Vinai,[2] D. Dagur,[2,3] and P. D. C. King[1,c)]

AFFILIATIONS

[1]SUPA, School of Physics and Astronomy, University of St Andrews, North Haugh, St Andrews KY16 9SS, United Kingdom
[2]Istituto Officina dei Materiali (IOM)-CNR, Laboratorio TASC, Area Science Park, S.S.14, Km 163.5, 34149 Trieste, Italy
[3]Department of Physics, University of Trieste, Trieste, Via Alfonso Valerio 2, Trieste 34127, Italy

[a)]**Author to whom correspondence should be addressed:** yn25@st-andrews.ac.uk
[b)]**Now at:** Synchrotron SOLEIL, 91190 Saint-Aubin, France.
[c)]**Electronic mail:** pdk6@st-andrews.ac.uk

ABSTRACT

$AgCrSe_2$ exhibits remarkably high ionic conduction, an inversion symmetry-breaking structural transition, and is host to complex non-colinear magnetic orders. Despite its attractive physical and chemical properties and its potential for technological applications, studies of this compound to date are focused almost exclusively on bulk samples. Here, we report the growth of $AgCrSe_2$ thin films via molecular beam epitaxy. Single-orientated epitaxial growth was confirmed by x-ray diffraction, while resonant photoemission spectroscopy measurements indicate a consistent electronic structure as compared to bulk single crystals. We further demonstrate significant flexibility of the grain morphology and cation stoichiometry of this compound via control of the growth parameters, paving the way for the targeted engineering of the electronic and chemical properties of $AgCrSe_2$ in thin-film form.

I. INTRODUCTION

Layered materials often exhibit useful and interesting properties, in part due to the prevalence of quantum size effects owing to their inherently restricted dimensionality. Among such systems, materials that form as "natural heterostructures," in which each layer contributes distinct properties, provide a unique playground to explore novel phenomena arising from interactions between the charge, spin, orbital, and structural degrees of freedom of the disparate subsystems. $AgCrSe_2$ is one such material, comprised of alternately stacked triangular-lattice $CrSe_2$ and Ag layers [Fig. 1(a)].[1] The $CrSe_2$ sublattice is analogous to the van der Waals (vdW) crystal $CrSe_2$,[2] which is currently under intense investigation as a possible host of two-dimensional magnetism.[3,4] Unlike the vdW compounds, however, additional Ag atoms are located between the $CrSe_2$ layers in $AgCrSe_2$, making this material a close relative to the Cr-based delafossite oxides, e.g., $AgCrO_2$.[5] In such delafossites, trivalent Cr ions (Cr^{3+}) with a $3d^3$ electron configuration half-fill the t_{2g} orbitals, giving rise to $S = \frac{3}{2}$ magnetism, which results in a frustrated anti-ferromagnetic order within the triangular Cr in-plane sublattice at low temperature,[6,7] and in $AgCrSe_2$, the formation of a half-metallic electron gas at the $CrSe_2$-terminated surface.[8]

There are two inequivalent Ag sites between these $CrSe_2$ layers, both forming triangular sublattices in $AgCrSe_2$. At room temperature, Ag atoms exclusively occupy only one of these sublattices, making the structure non-centrosymmetric [Fig. 1(b), bottom]. Upon heating, however, $AgCrSe_2$ exhibits an order–disorder transition. A significant increase in Ag ion mobility leads to a dynamical population of both Ag sublattices, which makes all Ag sites, on average, half-filled [Fig. 1(b), top], causing a symmetry change from R3m to $R\bar{3}m$ and restoring inversion symmetry.[1,9,10] Liquid-like thermal conduction has been reported on $AgCrSe_2$ in the superionic state,[11] where transverse vibrations of Ag atoms are suppressed by the ultrafast atomic fluctuations inherent to the order–disorder transition, resulting in extremely low lattice thermal conduction.

High ionic conductivity makes $AgCrSe_2$ an interesting candidate for investigation for use in solid fuel batteries, eliminating the

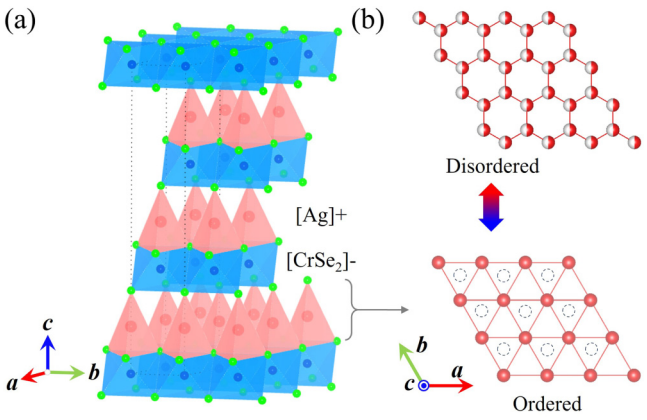

FIG. 1. (a) The room-temperature crystal structure of $AgCrSe_2$ where $CrSe_2$ layers and Ag layers are stacked alternately along the *c*-axis direction.[1] The lattice parameters reported for bulk crystals at room temperature are $a_{bulk} = 3.6798–3.6834$ Å, and $c_{bulk} = 21.210–21.231$ Å, respectively.[1,9,16] (b) Top view of the Ag sublattice in the ordered (bottom) and disordered (top) state. Two inequivalent configurations are possible for Ag atoms (red filled circles and circles with broken line). In the ordered state, Ag atoms predominantly occupy the former configuration while a thermally driven melting of this order allows both configurations with equal probability at high temperature.

use of flammable Li-based liquid electrolytes. Furthermore, the low thermal conductivity also gives this material group an advantageous position for other technological applications such as thermal insulation and efficient thermoelectric devices. This motivates developing approaches to stabilize $AgCrSe_2$ in thin-film geometries. For example, quantum confinement and the introduction of material interfaces, which effectively scatter phonons or serve to filter out the low-energy electrons at interfacial energy barriers, can provide a powerful route for enhancing thermoelectric figures of merit,[12] while there are several promising reports of tunable ionic and thermal conductivity via control of material thickness, grain size, and the formation of nanocomposites.[13–15] To date, however, such approaches have barely been applied to $AgCrSe_2$, and developing experimental pathways to control its crystal growth with nanoscale precision is strongly desired.

In this study, we have employed thin film synthesis using molecular beam epitaxy (MBE). This technique is known for its excellent controllability of the growth parameters, and thus its ability to fabricate thin films with high crystalline quality. Here, we report the first growth of $AgCrSe_2$ thin films and the characterization of their morphological and electronic properties.

II. EXPERIMENTAL DETAILS

All samples shown in this report were fabricated using molecular beam epitaxy (MBE) in a DCA Instruments R450 system. Elemental sources (Cr, Se, and Ag) were evaporated using an effusion cell, valved cracker cell, and electron-beam evaporator (Focus GmbH, UVH evaporator EFM 3T), respectively. Flux rates of each constituent element are controlled independently. As a standard growth condition, cell temperatures for Cr and Se are kept at 1050 and 150 °C (cell)/500 °C (cracker), respectively. The Ag flux is monitored in real time using a flux monitor, which provides a current value corresponding to the Ag flux. Due to the much higher vapor pressure of Se as compared to transition metal elements, the Se-to-metal flux ratio was kept more than ten times larger than the stoichiometric ratio in order to minimize Se deficiency in the films. Similarly, all samples were cooled in the Se environment (Se partial pressure $P_{Se} \approx 1 \times 10^{-7}$ mbar).

Selection of substrate materials is one of the most crucial parts of thin film synthesis. Unless otherwise stated, we employed highly orientated pyrolytic graphite (HOPG, MaTeck GmbH, epitaxial strain $\varepsilon \approx -30\%$) as a growth substrate for all the samples discussed here. This allows for growing quasi "free-standing" unstrained thin films via a van der Waals epitaxy-like growth,[17] in order to investigate the intrinsic behavior of $AgCrSe_2$. The HOPG substrates are freshly cleaved just before introducing them into a vacuum chamber. However, the in-plane polycrystalline nature of HOPG substrates makes them unsuitable to use for x-ray diffraction (XRD) measurements. We thus also fabricated a companion sample using a 6H-SiC (TankeBlue Co. Ltd.) substrate, which was thermally treated to form an overlayer of bi-layer graphene. In order to achieve enough signal intensity for accurate analysis for phase identification and crystal orientation, this sample has ≈ 8 times larger thickness compared to the other films studied here. In order to achieve this thickness in a feasible time, a slightly higher growth rate was used, with the Cr cell temperature set at 1100 °C. The substrates were all degassed prior to growth at 50 °C above the growth temperature for 10 min in vacuum.

Throughout the deposition, the surface morphology and the in-plane lattice spacing of the material are monitored with reflection high energy electron diffraction (RHEED, STAIB RH15), and *ex situ* x-ray diffraction (XRD, Bruker D8) was used to confirm the crystalline phase. Samples were also examined with x-ray absorption spectroscopy (XAS) and resonant photoemission spectroscopy (resPES) to probe the chemical environments of the constituent metal elements and the electronic structure of the resulting films. For these samples, we deposited an amorphous Se layer at room temperature, before removing the samples from vacuum for transport to APE-HE beamline at Elettra Sincrotrone, Trieste,[18] for the spectroscopic characterization. The Se capping layers were approximately 20 Å thick and were removed just before the measurements by heating the samples in vacuum up to desorption temperature of Se, in a similar manner described elsewhere.[19,20] The Se 3*d* XPS spectrum was constantly monitored during decapping to minimize the residual Se on the surface while preventing the decomposition of the phase. Atomic force microscopy (AFM, Park systems NX10) measurements were performed in a non-contact mode, to evaluate the surface morphology.

III. RESULTS AND DISCUSSIONS

Figure 2(a) shows RHEED image taken during the deposition of $AgCrSe_2$ on a graphene/SiC substrate (similar results were obtained for growth on HOPG substrates, see Fig. S1 in the supplementary material). Clear and sharp diffraction streaks are obtained from the growing epilayer (orange arrows), indicating a relatively smooth and well-ordered surface. In addition, a faint

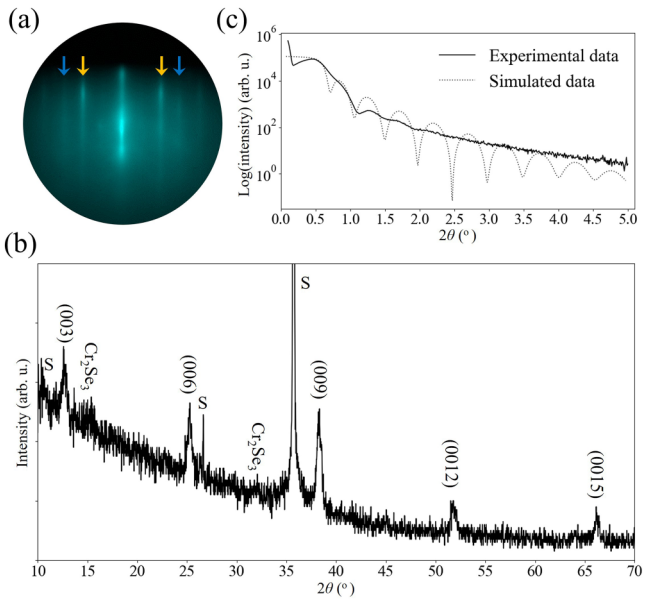

FIG. 2. (a) RHEED image during the growth of $AgCrSe_2$ on a bi-layer graphene/SiC substrate, taken 10 min after starting the deposition, for an estimated film thickness of ≈7 Å. Diffraction patterns originating from substrate and epilayer are indicated with blue and orange arrows, respectively. (b) 2θ-ω XRD pattern of the same sample shown in (a). The indexed peaks are diffraction from $AgCrSe_2$ (0 0 3*l*) planes along with substrate-related peaks (denoted as S), indicating epitaxial growth of singly orientated $AgCrSe_2$. On the other hand, small signals related to Cr_2Se_3 were observed too; this may imply a finite amount of Ag deficiency in the film. (c) XRR profile of the same sample as shown in (b). Compared to a simulated curve for a $AgCrSe_2$ film with smoother surface (shown as a gray dotted curve), the experimental data show a strongly damped oscillation, suggesting a non uniform, rough film surface.

diffraction pattern is observed corresponding to the growth substrate, which eventually disappears as the coverage and film thickness are increased. The in-plane lattice constants estimated from our RHEED measurements range from 3.56 to 3.83 Å, and there were no significant differences between in-plane lattice constants of films grown on HOPG and those on graphene/SiC. Including samples grown on both types of substrates, we obtained an average value of 3.66 Å. This value is comparable to, although slightly smaller than, typical values reported for bulk crystals of $AgCrSe_2$ (a_{bulk} = 3.6798–3.6834 Å[1,9,16]). The variation of in-plane lattice constants can be attributed to some off-stoichiometry in the film composition, as discussed in more detail below.

We show XRD measurement (2θ-ω scan) of a companion sample grown on an epitaxial graphene/SiC substrate in Fig. 2(b). In addition to the SiC substrate, sharp peaks related to (0 0 3*l*) planes of $AgCrSe_2$ can be clearly resolved, indicating the coherent growth of *c*-axis orientated $AgCrSe_2$. We note that the difference in the lattice constant between the two known bulk polymorphs of $AgCrSe_2$ [Fig. 1(b)] is less than 0.1%. It is therefore not possible to distinguish the crystal symmetry solely based on the XRD results presented here, and we thus hope that our work will serve as a motivation for future detailed structural studies in the future. We can still extract some basic materials' parameters from these measurements. In particular, the *c*-axis lattice constant, derived by Nelson–Reily fitting to the peak positions,[21] is 21.17 ± 0.06 Å, again slightly shorter yet comparable to the values reported for bulk crystals (c_{bulk} = 21.210–21.231 Å[1,9,16]). On the other hand, small signals from Cr_2Se_3 impurity phase can also be seen, suggesting propensity for the inclusion of regions of Ag-poor off-stoichiometry. The film thickness was estimated from fitting to the x-ray reflectivity (XRR) profile to be ≈ 16.8 nm, while a damped oscillation can be observed too [Fig. 2(c)] which typically reflects some non-uniformity and roughening on the film surface. Atomic force microscopy (AFM) measurements on this sample confirm a rather rough surface morphology of the as-grown epilayers, with root mean square roughness of ≈ 4.4 nm.

The reduced lattice parameters as compared to bulk $AgCrSe_2$ and the presence of residual Cr_2Se_3 inclusions likely reflect a finite Ag deficiency in our grown films. Indeed, Ag vacancies are also known to be a prevalent cause of off-stoichiometry in the synthesis of bulk samples.[22] To explore this further, and to investigate the possibility of deliberate tuning of the chemical and physical properties in $AgCrSe_2$ thin films, we have systematically varied the growth temperature (T_s) and Ag flux during the growth. Figure 3(a) shows AFM images of films grown with a range of substrate temperatures and incident Ag flux, while the Cr and Se fluxes and the growth duration were kept unchanged. The film growth proceeds, in all cases, via the formation of relatively small crystalline grains. As the growth temperature increases, these grains become larger, transforming from randomly formed islands to thermodynamically preferred triangular/hexagonal islands, with smoother surfaces. Consistent with this, we find that the measured RHEED patterns from these samples (see Fig. S2 in the supplementary material) exhibit sharper film streaks for samples grown at higher temperatures and with lower Ag fluxes. To quantify this, we have estimated the crystallographic correlation length from the measured full width at half maximum (FWHM) of the film streaks from line cuts through our RHEED images, taken after cooling to room temperature. The correlation length is plotted as a function of growth temperature and Ag flux in Fig. 3(b). Similar to the trend on the surface morphology shown in Fig. 3(a), it is clear from these how higher growth temperature generally acts to increase the correlation length while lowering the Ag flux also provides an additional contribution to improving the crystal quality. This largely reflects an increase in the atomic mobility with increasing growth temperature. Moreover, by reducing the Ag flux, we find a slight reduction of the film coverage which appears to indicate that the growth rate of $AgCrSe_2$ is limited by the Ag supply in this regime. Thus, the improved island morphology for lower Ag flux likely reflects the effects of the reduced growth rate, which in turn effectively increases the time available for both surface and edge diffusion. These tendencies qualitatively match with the previously reported trend on the epitaxial growth of various binary transition metal dichalcogenides,[23] suggesting a universal scheme for controlling grain morphology in thin film growth of both binary and complex transition metal chalcogenide systems.

From these studies, it is evident that higher growth temperature is advantageous for the formation of smooth and larger

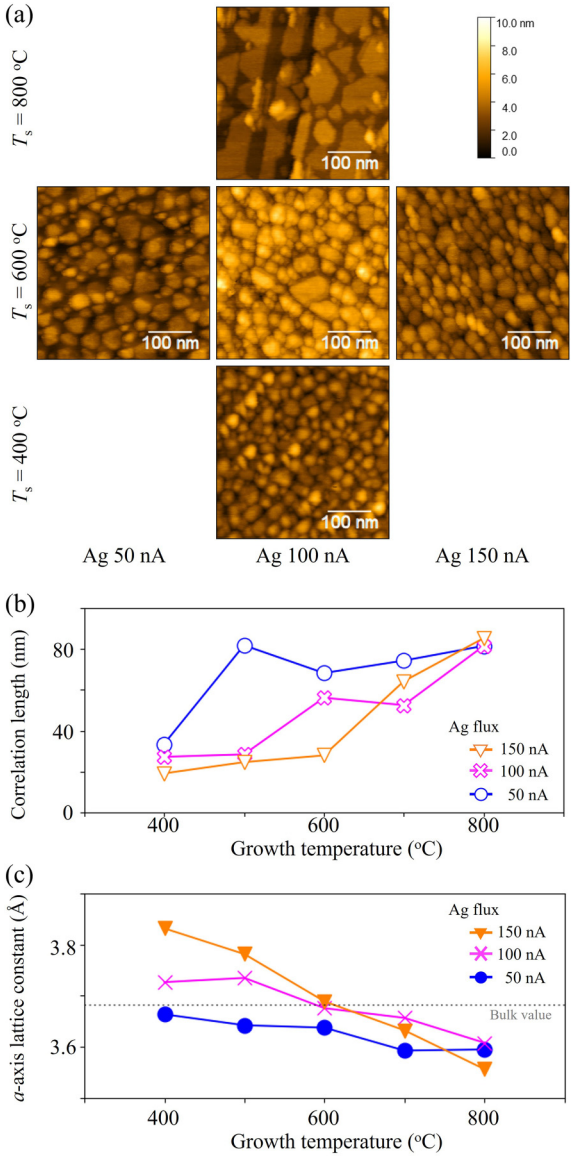

FIG. 3. (a) AFM images of $AgCrSe_2$ thin films grown on HOPG substrates, using different growth temperature (T_s) and Ag flux. All images are in the same $0.4 \times 0.4\,\mu m^2$ scale with 205 px × 205 px resolution. As the growth temperature increases (from bottom to top in the figure), the grain shape changes from a random rounded shape to thermodynamically favored triangular/hexagonal shapes. Lowering the Ag flux (from right to left) brings similar changes as well as a slight reduction in the film coverage, implying reduction of growth rate leading to enhanced surface and edge diffusion. (b) Crystallographic correlation length and (c) *a*-axis lattice constants of $AgCrSe_2$ thin films on HOPG, derived from RHEED images at room temperature (see Fig. S2 in the supplementary material). The in-plane lattice constant of bulk samples (Ref. 1) is shown as a horizontal gray line in (c). Similar to the grain morphology visible in the AFM images, the estimated correlation lengths increase when using higher growth temperature and lower Ag flux, reflecting improved crystal quality, while these growth parameters also influence the film composition resulting in a range of in-plane lattice constants.

surfaces of $AgCrSe_2$ thin films. However, it also affects the film composition. In Fig. 3(c), we show the *a*-axis lattice constants of the same films shown in Fig. 3(b), as similarly derived from RHEED images. In particular, we find that the *a*-axis parameter reduces with increasing growth temperature, which corresponds to a reduced Ag-to-Cr ratio in the films.[22] This can be understood from the relative vapor pressures of the constituent elements, with the vapor pressure of Ag 3–4 orders of magnitude higher than that of Cr in the temperature range used for the film growth.[24,25] This makes the formation of intrinsic Ag vacancies more likely to occur, particularly at the higher growth temperatures, promoting the desorption of Ag atoms from the film surface. We find, however, that this Ag loss can at least partially be compensated by increasing the Ag flux supplied during the growth, driving a tendency for the lattice constant to increase. This is particularly pronounced for lower growth temperatures, while negligible changes with Ag flux are observed at the highest growth temperatures studied here. We attribute this different behavior to the relatively high vapor pressure of Ag, with increased desorption likely at the higher growth temperatures. This therefore suggests that Ag deficiency can be suppressed both by supplying excess Ag to compensate the Ag loss and by slightly lowering the growth temperature. In fact, at the lowest growth temperatures and highest Ag fluxes, we find lattice constants even larger than in bulk crystals, where Ag deficiency is still known to be common. We note, however, the complex interplay with the morphology of the sample as discussed above. Different parameter regimes of stoichiometry and morphology, therefore, appear possible. In particular, as the growth temperature is the primary factor to determine grain morphology (both size and shape), we propose that Ag flux can then be used as the main tuning parameter to control the growth rate and composition of $AgCrSe_2$, i.e., Ag vacancy concentration, with moderately higher growth temperatures maintained to optimize the film morphology.

Having established the possibility to stabilize phase-pure $Ag_{1-\delta}CrSe_2$ in thin-film form, we now investigate the electronic structure of such samples. We show in Fig. 4(a) XAS measurements with linear horizontal polarization at the Cr $L_{2,3}$ edge. The spectrum shown here is in good agreement with the characteristic profile of Cr^{3+} in ionic systems, except that the multiplet structure is smeared out as compared to, e.g., Cr^{3+}-based oxides.[26] This suggests higher charge transfer and a more covalent nature of Cr–Se bonding in this system,[27–31] with our measurements in excellent agreement with XAS measurements from bulk $AgCrSe_2$ samples.[8,32]

In Fig. 4(b), we show the valence band photoemission spectra measured in the soft x-ray regime. A broad valence bandwidth of ≈8 eV is found, with negligible spectral weight at the Fermi level. This indicates that our films are semiconducting, but with the Fermi level located close to the top of the valence band, as is also the case for bulk $AgCrSe_2$.[32] Two pronounced peaks in the valence band density of states (VB-DOS) are observed at around 1–2 eV and 6 eV below the Fermi level. To probe the elemental contribution of these, we measured the VB-DOS as the photon energy is tuned across the Cr $L_{2,3}$ x-ray absorption edges [resonant photoemission (resPES)], where the spectral weight from Cr-derived states is enhanced as the probing photon energy is tuned into resonance with the dipole-allowed core-to-valence transition. A clear increase in spectral weight of the peak at $E - E_F \approx -2$ eV allows us

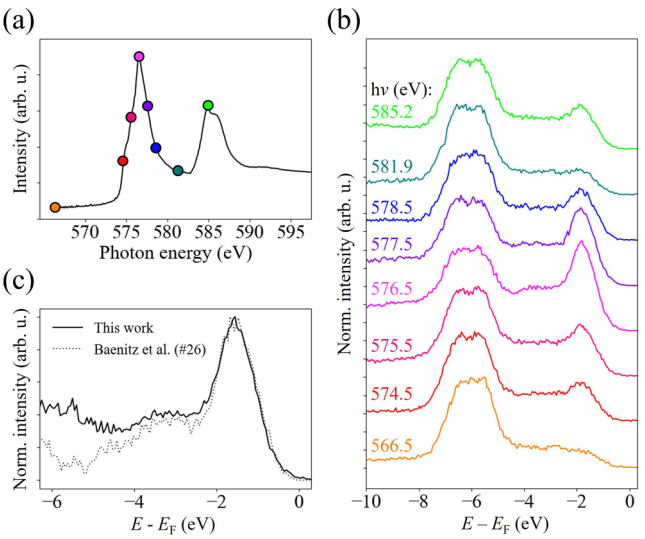

FIG. 4. (a) Cr $L_{2,3}$-edge XAS measurements and (b) resPES measurements from a $AgCrSe_2$ thin film grown on an HOPG substrate with a film thickness of ≈20 Å. The colors of the filled circles on the XAS profile indicate photon energies where resPES measurements were taken. (c) Cr partial density of states (PDOS) calculated by subtracting the off-resonant spectra (hν = 566.5 eV) from the on-resonant one (hν = 576.5 eV). The resulting Cr PDOS closely matches that observed in similar measurements from bulk single crystal $AgCrSe_2$ (gray line).[32]

to assign this peak as arising due to Cr-derived states, while the weight of the peak at ≈ −6 eV binding energy remains rather constant with changing photon energy. We thus attribute this to Ag-derived states, consistent with the nominal Ag^{1+} charge state, and a d^{10} electron configuration of the Ag layers. These states should be rather localized here, and they thus give rise to a substantial contribution to the DOS.

To assess the degree of hybridization of the Cr and Se states, we show the Cr partial DOS, extracted as the difference of photoemission spectra measured on and off resonance, in Fig. 4(c). This shows non-negligible Cr weight over an extended energy range throughout the DOS, pointing to significant Cr–Se hybridization, consistent with our XAS measurements discussed above. Indeed, our resPES spectra are in excellent agreement with those previously obtained from bulk $AgCrSe_2$ single crystal samples[32] [Fig. 4(c)]. This not only provides additional support to our structural characterizations performed above, but further indicates that the electronic structure of $AgCrSe_2$ thin films remains largely unchanged from those of the bulk compound, at least at the thickness range we have investigated here.

IV. CONCLUSION

In summary, we have systematically investigated the growth window for epitaxial growth of $AgCrSe_2$ thin films by means of molecular beam epitaxy. We have demonstrated the possibility for tuning both the surface morphology and stoichiometry, in particular, the amount of Ag deficiency, by varying the growth temperature and the Ag flux used during the growth. From x-ray absorption spectroscopy and resonant photoemission, we have shown that our samples support a nominal Cr^{3+} valence and an electronic structure markedly similar to that of the bulk single crystal, suggesting thin films of $AgCrSe_2$ as an ideal platform in which to investigate, and attempt to control, the magnetic order on the Cr sites, as well as to explore the influence of cation off-stoichiometry on superionic conduction in this system.

SUPPLEMENTARY MATERIAL

See the supplementary material for the comparison of RHEED images between $AgCrSe_2$ thin films grown on two different substrates, i.e., HOPG and graphene/SiC (Fig. S1) and $AgCrSe_2$ films grown on HOPG with varied growth temperature as well as Ag flux (Fig. S2).

ACKNOWLEDGMENTS

We thank Gesa Siemann, Haijing Zhang, Helge Roesner, and Michael Baenitz for useful discussions and Edvard Dobovicnik for development work at the APE-HE beamline. The authors gratefully acknowledge the European Research Council (through the QUESTDO project, No. 714193) and The Leverhulme Trust (Grant No. RL-2016-006) for support. The MBE growth facility was funded through an EPSRC strategic equipment Grant (Grant No. EP/M023958/1). We acknowledge Elettra Sincrotrone Trieste for providing access to its synchrotron radiation facilities through Proposal No. 20215618. The research leading to this result has been supported by the project CALIPSO under Grant Agreement No. 312284 from the EU Seventh Framework Programme (FP7/2007-2013). Part of this work has been performed in the framework of the Nanoscience Foundry and Fine Analysis (NFFA-MUR Italy Progetti Internazionali) project. Schematics of crystal structure were made by using VESTA.[33] For the purpose of open access, the authors have applied a Creative Commons Attribution (CC BY) license to any Author Accepted Manuscript version arising.

AUTHOR DECLARATIONS

Conflict of Interest

The authors have no conflicts to disclose.

Author Contributions

Y. Nanao: Data curation (equal); Formal analysis (equal); Investigation (equal); Software (equal); Writing – original draft (equal); Writing – review & editing (equal). **C. Bigi:** Data curation (equal); Formal analysis (supporting); Software (supporting); Writing – review & editing (supporting). **A. Rajan:** Data curation (supporting); Writing – review & editing (supporting). **G. Vinai:** Data curation (supporting); Writing – review & editing (supporting). **D. Dagur:** Data curation (supporting); Writing – review & editing (supporting). **P. D. C. King:** Funding acquisition (equal); Project administration (equal); Resources (equal); Supervision (equal); Writing – review & editing (equal).

DATA AVAILABILITY

The data that support the findings of this study are openly available in University of St Andrews research information system (PURE), at https://doi.org/10.17630/b0744432-adc7-4bd7-bed3-2eb6fdf58e72, Ref. 34.

REFERENCES

[1]F. Engelsman, G. Wiegers, F. Jellinek, and B. Van Laar, "Crystal structures and magnetic structures of some metal (I) chromium (III) sulfides and selenides," J. Solid State Chem. **6**, 574–582 (1973).

[2]C. Van Bruggen, R. Haange, G. Wiegers, and D. De Boer, "$CrSe_2$, a new layered dichalcogenide," Physica B+C **99**, 166–172 (1980).

[3]B. Li, Z. Wan, C. Wang, P. Chen, B. Huang, X. Cheng, Q. Qian, J. Li, Z. Zhang, G. Sun, and B. Zhao, "Van der Waals epitaxial growth of air-stable $CrSe_2$ nanosheets with thickness-tunable magnetic order," Nat. Mater. **20**, 818–825 (2021).

[4]L. Wu, L. Zhou, X. Zhou, C. Wang, and W. Ji, "In-plane epitaxy-strain-tuning intralayer and interlayer magnetic coupling in $CrSe_2$ and $CrTe_2$ monolayers and bilayers," Phys. Rev. B **106**, L081401 (2022).

[5]E. Gehle and H. Sabrowsky, "Zur darstellung und kristallstruktur von $AgCrO_2$/synthesis and crystal structure of $AgCrO_2$," Z. Naturforsch. B **30**, 659–661 (1975).

[6]Y. Oohara, S. Mitsuda, H. Yoshizawa, N. Yaguchi, H. Kuriyama, T. Asano, and M. Mekata, "Magnetic phase transition in $AgCrO_2$," J. Phys. Soc. Jpn. **63**, 847–850 (1994).

[7]S. Seki, Y. Onose, and Y. Tokura, "Spin-driven ferroelectricity in triangular lattice antiferromagnets $ACrO_2$ (A = Cu, Ag, Li, or Na)," Phys. Rev. Lett. **101**, 067204 (2008).

[8]G.-R. Siemann, S.-J. Kim, E. A. Morales, P. A. Murgatroyd, A. Zivanovic, B. Edwards, I. Marković, F. Mazzola, L. Trzaska, O. J. Clark, and C. Bigi, "Spin-orbit coupled spin-polarised hole gas at the $CrSe_2$-terminated surface of $AgCrSe_2$," npj Quantum Mater. **8**, 1–7 (2023).

[9]A. Van Der Lee and G. Wiegers, "Anharmonic thermal motion of Ag in $AgCrSe_2$: A high-temperature single-crystal X-ray diffraction study," J. Solid State Chem. **82**, 216–224 (1989).

[10]D. Murphy, H. Chen, and B. Tell, "Superionic conduction in $AgCrS_2$ and $AgCrSe_2$," J. Electrochem. Soc. **124**, 1268 (1977).

[11]B. Li, H. Wang, Y. Kawakita, Q. Zhang, M. Feygenson, H. Yu, D. Wu, K. Ohara, T. Kikuchi, K. Shibata, and T. Yamada, "Liquid-like thermal conduction in intercalated layered crystalline solids," Nat. Mater. **17**, 226–230 (2018).

[12]M. S. Dresselhaus, G. Chen, M. Y. Tang, R. Yang, H. Lee, D. Wang, Z. Ren, J.-P. Fleurial, and P. Gogna, "New directions for low-dimensional thermoelectric materials," Adv. Mater. **19**, 1043–1053 (2007).

[13]J. Peng, Y. Liu, H. Lv, Y. Li, Y. Lin, Y. Su, J. Wu, H. Liu, Y. Guo, Z. Zhuo, and X. Wu, "Stoichiometric two-dimensional non-van der Waals $AgCrS_2$ with superionic behaviour at room temperature," Nat. Chem. **13**, 1235–1240 (2021).

[14]S. Bhattacharya, A. Bohra, R. Basu, R. Bhatt, S. Ahmad, K. Meshram, A. Debnath, A. Singh, S. K. Sarkar, M. Navneethan, and Y. Hayakawa, "High thermoelectric performance of $(AgCrSe_2)_{0.5}(CuCrSe_2)_{0.5}$ nano-composites having all-scale natural hierarchical architectures," J. Mater. Chem. A **2**, 17122–17129 (2014).

[15]Y. Wang, Y. Wang, C. Chen, K. Koumoto, S. He, and L. Pan, "Remarkable effects of shear-exfoliation and restacking on microstructural texturing and thermoelectric properties of $AgCrSe_2$," J. Alloys Compd. **958**, 170504 (2023).

[16]U. K. Gautam, R. Seshadri, S. Vasudevan, and A. Maignan, "Magnetic and transport properties, and electronic structure of the layered chalcogenide $AgCrSe_2$," Solid State Commun. **122**, 607–612 (2002).

[17]Y.-H. Chu, "Van der Waals oxide heteroepitaxy," npj Quantum Mater. **2**, 67 (2017).

[18]G. Panaccione, I. Vobornik, J. Fujii, D. Krizmancic, E. Annese, L. Giovanelli, F. Maccherozzi, F. Salvador, A. De Luisa, D. Benedetti *et al.*, "Advanced photoelectric effect experiment beamline at Elettra: A surface science laboratory coupled with synchrotron radiation," Rev. Sci. Instrum. **80**, 043105 (2009).

[19]D. Drews, A. Schneider, D. Zahn, D. Wolfframm, and D. Evans, "Raman monitoring of selenium decapping and subsequent antimony deposition on MBE-grown ZnSe (100)," Appl. Surf. Sci. **104**, 485–489 (1996).

[20]G. Vinai, C. Bigi, A. Rajan, M. D. Watson, T.-L. Lee, F. Mazzola, S. Modesti, S. Barua, M. C. Hatnean, G. Balakrishnan, and P. D. C. King, "Proximity-induced ferromagnetism and chemical reactivity in few-layer VSe_2 heterostructures," Phys. Rev. B **101**, 035404 (2020).

[21]J. B. Nelson and D. Riley, "An experimental investigation of extrapolation methods in the derivation of accurate unit-cell dimensions of crystals," Proc. Phys. Soc. **57**, 160 (1945).

[22]M. Tang, Z. Chen, C. Yin, L. Lin, D. Ren, B. Liu, B. Kang, and R. Ang, "Thermoelectric modulation by intrinsic defects in superionic conductor Ag_xCrSe_2," Appl. Phys. Lett. **116**, 163901 (2020).

[23]A. Rajan, K. Underwood, F. Mazzola, and P. D. King, "Morphology control of epitaxial monolayer transition metal dichalcogenides," Phys. Rev. Mater. **4**, 014003 (2020).

[24]M. B. Panish, "Vapor pressure of silver," J. Chem. Eng. Data **6**, 592–594 (1961).

[25]E. Gulbransen and K. Andrew, "A preliminary study of the oxidation and vapor pressure of chromium," J. Electrochem. Soc. **99**, 402 (1952).

[26]S. Fiori, D. Dagur, M. Capra, A. Picone, A. Brambilla, P. Torelli, G. Panaccione, and G. Vinai, "Electronically ordered ultrathin Cr_2O_3 on Pt (1 1 1) in presence of a multidomain graphene intralayer," Appl. Surf. Sci. **613**, 155918 (2023).

[27]A. Frisk, L. B. Duffy, S. Zhang, G. van der Laan, and T. Hesjedal, "Magnetic X-ray spectroscopy of two-dimensional CrI_3 layers," Mater. Lett. **232**, 5–7 (2018).

[28]Y. S. Dedkov, A. Vinogradov, M. Fonin, C. König, D. Vyalikh, A. Preobrajenski, S. Krasnikov, E. Y. Kleimenov, M. Nesterov, U. Rüdiger, and S. L. Molodtsov, "Correlations in the electronic structure of half-metallic ferromagnetic CrO_2 films: An x-ray absorption and resonant photoemission spectroscopy study," Phys. Rev. B **72**, 060401 (2005).

[29]V. Sunko, F. Mazzola, S. Kitamura, S. Khim, P. Kushwaha, O. Clark, M. Watson, I. Marković, D. Biswas, L. Pourovskii, and T. K. Kim, "Probing spin correlations using angle-resolved photoemission in a coupled metallic/Mott insulator system," Sci. Adv. **6**, eaaz0611 (2020).

[30]D. Meyers, S. Mukherjee, J.-G. Cheng, S. Middey, J.-S. Zhou, J. Goodenough, B. Gray, J. Freeland, T. Saha-Dasgupta, and J. Chakhalian, "Zhang-Rice physics and anomalous copper states in A-site ordered perovskites," Sci. Rep. **3**, 1–5 (2013).

[31]J.-S. Kang, G. Kim, H. Lee, H. Kim, D. Kim, S. Han, S. Kim, C. Kim, H. Lee, J.-Y. Kim, and B. I. Min, "Synchrotron radiation spectroscopy study of $FeCr_2X_4$ (X = S and Se)," J. Appl. Phys. **103**, 07D717 (2008).

[32]M. Baenitz, M. Piva, S. Luther, J. Sichelschmidt, K. Ranjith, H. Dawczak-Dębicki, M. Ajeesh, S.-J. Kim, G. Siemann, C. Bigi, and P. Manuel, "Planar triangular $S = 3/2$ magnet $AgCrSe_2$: Magnetic frustration, short range correlations, and field-tuned anisotropic cycloidal magnetic order," Phys. Rev. B **104**, 134410 (2021).

[33]K. Momma and F. Izumi, "Vesta 3 for three-dimensional visualization of crystal, volumetric and morphology data," J. Appl. Crystallogr. **44**, 1272–1276 (2011).

[34]Y. Nanao, C. Bigi, A. Rajan, G. Vinai, D. Dagur, and P. D. C. King (2024). "Epitaxial growth of $AgCrSe_2$ thin films by molecular beam epitaxy" https://doi.org/10.17630/b0744432-adc7-4bd7-bed3-2eb6fdf58e72.